

## Localization of shadow poles by complex scaling

Attila Csóttó\*

*Institute of Nuclear Research of the Hungarian Academy of Sciences, P.O. Box 51, Debrecen, H-4001, Hungary*

(Received 5 May 1993)

Through numerical examples, we show that the complex-scaling method is suited to explore the pole structure in multichannel scattering problems. All poles lying on the multisheeted Riemann energy surface, including shadow poles, can be revealed and the Riemann sheets on which they reside can be identified.

PACS number(s): 34.10.+x, 24.10.Eq, 24.30.Gd

Resonant states are solutions of the Schrödinger equation with outgoing asymptotic boundary condition. It was pointed out long ago that these solutions must belong to complex eigenenergies and the scattering matrix has poles at these energies [1]. In the coordinate-space, resonant eigenfunctions show oscillatory behavior in the asymptotic region, with exponentially growing amplitude,  $\sim \exp[i(\kappa - i\gamma)r]$  ( $\kappa, \gamma > 0$ ), thus, they are not elements of the  $L^2$  space. Complex scaling is a most powerful and easily applicable method to describe such states [2–4]. It has been successfully applied in atomic [2, 5] and nuclear physics [5–7].

In single-channel problems the working mechanism of the complex-scaling method (CSM) is well understood and there is almost no obscure point. The situation is not so clear, however, in multichannel cases. The pole structure of a multichannel scattering matrix is much more complicated than that of a single-channel  $S$  function. In the case of Hermitian potentials, a pole that would appear in one of the  $N$  channels in a single-channel problem, gives rise to  $2^{N-1}$  poles on different Riemann energy sheets in the coupled  $N$ -channel problem [8, 9]. The easiest way to label a Riemann sheet is to give the signs of the imaginary parts of the channel wave numbers  $k_i$  ( $i = 1, 2, \dots, N$ ) in an  $N$ -term sign string [ $\text{sgn}(\text{Im } k_1), \text{sgn}(\text{Im } k_2), \dots, \text{sgn}(\text{Im } k_N)$ ] [10]. In the zero-coupling limit, all  $2^{N-1}$  poles are at the same energy position on different sheets, while, by varying the coupling strengths, the poles move, and a crossing of the real energy axis by one of them implies a crossing over to another Riemann sheet. It has been a long-standing belief that only those poles (named ordinary poles) can have appreciable effects on the physically observable quantities which are on the Riemann sheet adjacent to the physical one. Recently, the effect of other poles, the so-called shadow poles, of the multichannel scattering matrix on some physical observables has attracted interest in atomic [11], particle [12], and nuclear physics [10, 13]. It turned out that in certain cases the shadow poles can cause strong effects; e.g., it is a shadow pole which causes the very large cross section of the famous  $d+t \rightarrow \alpha+n$  thermonuclear reaction [10, 13]. The effect of a shadow pole on the scattering matrix depends crucially on which Riemann sheet it is situated [9, 10, 13].

Although most of the applications of the CSM are in

multichannel problems, up until now all investigations have been concerned with ordinary poles. In this Brief Report we show that, using the CSM, one can search for poles on different Riemann sheets and can identify the poles by their sheets.

In a one-channel case the essence of the CSM is as follows. Instead of the

$$\hat{H}|\Psi\rangle = (\hat{T} + \hat{V})|\Psi\rangle = E|\Psi\rangle \quad (1)$$

eigenequation of the Hamiltonian  $\hat{H}$ , we solve the eigenvalue problem of the transformed Hamiltonian  $\hat{H}_\theta = \hat{U}(\theta)\hat{H}\hat{U}^{-1}(\theta)$ :

$$\hat{H}_\theta|\Psi_\theta\rangle = E_\theta|\Psi_\theta\rangle \quad (2)$$

(the  $\theta$  subscript of  $\Psi$  means that the wave function implicitly depends on  $\theta$ ; Hamiltonians with different  $\theta$  result in different wave functions).  $\hat{U}(\theta)$  is an unbounded similarity transformation [14], which, in the coordinate space, acts on a function  $f(r)$  such that

$$\hat{U}(\theta)f(r) = e^{3i\theta/2}f(re^{i\theta}). \quad (3)$$

[If  $\theta$  is real,  $U(\theta)$  means a rotation into the complex coordinate plane, if it is complex, it means a rotation and scaling.] The two problems are connected by the Aguilar-Balslev-Combes (ABC) theorem [15]. If  $\hat{V}$  is a (dilation) analytic operator, then (i) the bound eigenstates of  $\hat{H}$  are the eigenstates of  $\hat{H}_\theta$ , regardless of the actual value of  $\theta$ , within  $0 \leq \theta < \pi/2$ ; (ii) the continuous spectrum of  $\hat{H}$  will be rotated by an angle  $2\theta$ ; and (iii) a complex generalized eigenvalue of Eq. (2),  $E_{\text{res}} = \varepsilon - i\frac{1}{2}\Gamma$ ,  $\varepsilon, \Gamma > 0$  (with the wave number  $k_{\text{res}} = \kappa - i\gamma$ ,  $\kappa, \gamma > 0$ ), belongs to the proper spectrum of  $\hat{H}_\theta$  provided  $2\theta > |\arg E_{\text{res}}|$ .

Roughly speaking, the complex scaling transformation changes the asymptotic wave function from  $\exp[i(\kappa - i\gamma)r]$  to  $\exp[i(\kappa - i\gamma)r \exp(i\theta)]$ , which, in the case of  $2\theta > |\arg E_{\text{res}}| = 2|\arg k_{\text{res}}|$ , makes the diverging wave function localized. It is important to note that, if the sign of  $k_{\text{res}}$  is reversed, then the outgoing wave with  $\theta = 0$  is localized, and the complex scaling spoils the localization unless  $2\theta < |\arg E_{\text{res}}|$ . In a single-channel problem with a Hermitian potential  $-k_{\text{res}}$  is on the physical sheet,

where there are no resonance poles, but in a multichannel problem the imaginary parts of some channel wave numbers may be positive.

In multichannel cases Eq. (1) becomes a matrix equation

$$\sum_{\beta=1}^N \hat{H}_{\alpha\beta} |\Psi^\beta\rangle = E_\alpha |\Psi^\alpha\rangle, \quad \alpha = 1, 2, \dots, N, \quad (4)$$

where the Greek letters are the channel indices. The transformation operator of Eq. (3) becomes

$$\hat{U}_{\alpha\beta}(\theta) = \delta_{\alpha\beta} \hat{U}(\theta). \quad (5)$$

In the literature there are some hints on the strange behavior of the CSM in multichannel cases; e.g., in [16] the authors found that varying the rotation angle  $\theta$ , channel continua can absorb resonances that were revealed before, however, they did not explain this phenomenon. In [4] it is stated that such a phenomenon becomes transparent if one studies the multichannel problem on the Riemann energy surface, but no attempt has been made to assign these poles to Riemann sheets.

Here we study the working mechanism of the multichannel CSM in a simple model, which is easy to comprehend and control. Our model consists of a target with two internal states, whose thresholds are  $E_1$  and  $E_2$ , respectively, and a projectile. The two target states are the two channels. We choose one-term separable potentials [17] for both the diagonal and interchannel interactions,

$$\hat{V}_{\alpha\beta} = |\varphi_0^\alpha(b)\rangle \lambda_{\alpha\beta} \langle \varphi_0^\beta(b)|, \quad \alpha, \beta = 1, 2, \quad (6)$$

where  $|\varphi_0(b)\rangle$  is the eigenfunction of the three dimensional harmonic oscillator with  $n = 0$  oscillator quantum,  $b$  is the size parameter, and  $\lambda_{\alpha\beta}$  are the (real) potential strengths ( $\lambda_{12} = \lambda_{21}$ ). For the wave functions  $|\Psi_\theta^\gamma\rangle$  of (2), we use the following trial functions:

$$|\Psi_\theta^\gamma\rangle = \sum_{i=0}^{n_\gamma} c_{\gamma i} |\varphi_i^\gamma(\bar{b})\rangle, \quad \gamma = 1, 2 \quad (7)$$

in a variational method for the expansion coefficients  $c_i$  [this is the well-known wave-function expansion method]. With this ansatz, functions  $|\Psi_\theta^\gamma\rangle \in L^2$  are selected. The use of harmonic oscillator functions both in (6) and (7) makes it possible to calculate all necessary matrix elements analytically [17]. We choose size parameters in (7) different from that in (6) so as to make the trial function more flexible. If we set the strength of one of the diagonal interactions to be zero, the selected channel cannot accommodate a resonance, so that all poles we find in the coupled-channel problem must originate from the other channel, which implies that the sign belonging to the other channel must be negative. For the sake of simplicity, we take  $s$ -wave states throughout; although, the analytical expressions of [17] can be used for  $l \neq 0$  as well.

As a first example, we choose  $\lambda_{22} = 0$ ,  $\lambda_{11} = 1.0$ ,  $b = 0.6$ ,  $\bar{b} = 2.0$ ,  $E_1 = 0$ , and  $E_2 = 2$  (we use atomic units  $\hbar = m = 1$ ). The basis sizes ( $n_1, n_2$ ) are chosen so as to reach stable convergence. In the uncoupled

case ( $\lambda_{12} = \lambda_{21} = 0$ ) only one resonance pole appears at  $E = 3.049 - i2.153$  [Fig. 1(a)]. Switching on the coupling ( $\lambda_{12} = \lambda_{21} = 1.0$ ), we get different pole arrangements at different rotation angles [Figs. 1(b)–1(d)]. We can see in all figures that the poles distort the continua, as if they attracted or repelled the continuum points. This phenomenon has surfaced several times earlier, e.g., Refs. [6, 18], but as far as the author knows, it is as yet unexplained. Furthermore, we emphasize that in this work the central question is the working mechanism of the CSM in multichannel problems, which requires the use of very different rotation angles. Thus we do not perform an optimization in the  $\theta$  parameter (which could be done by choosing the stationary point of the  $\theta$  trajectory, see, e.g., [6]). These figures show the appearance and disappearance of poles, the same phenomenon as was mentioned above. The choice  $\lambda_{22} = 0$  and the fact that in the uncoupled case there is only one resonance pole guarantees that in this problem there is a pole on the  $(--)$  Riemann sheet and another, a shadow pole, on  $(-+)$  [9]. The pole at  $4.742 - i1.810$  is revealed only when both continua have swept over this point, which implies that the condition  $2\theta > |\arg E_{\text{res}}^\gamma|$ ,  $\gamma = 1, 2$  must be fulfilled in both channels (where  $E_{\text{res}}^1$  and  $E_{\text{res}}^2$  are the channel energies). Consequently, this pole is on the  $(--)$  sheet. For the other pole, which is on the  $(-+)$  sheet at  $2.395 - i1.467$ , the relations  $2\theta > |\arg E_{\text{res}}^1|$  and  $2\theta < |\arg E_{\text{res}}^2|$  must hold (cf. the remark after the ABC theorem, above). This is in full agreement with what we can see in the figures.

This example tells us that, if a pole is revealed, then it is on a Riemann sheet which is characterized by negative signs for all channels whose continua have swept over the pole, and positive signs for all others. A pole at  $E$  is an ordinary one (i.e., it is on a sheet adjacent to the physical sheet) if it has been swept over by the continua of all channels whose threshold energies are lower than  $\text{Re}(E)$

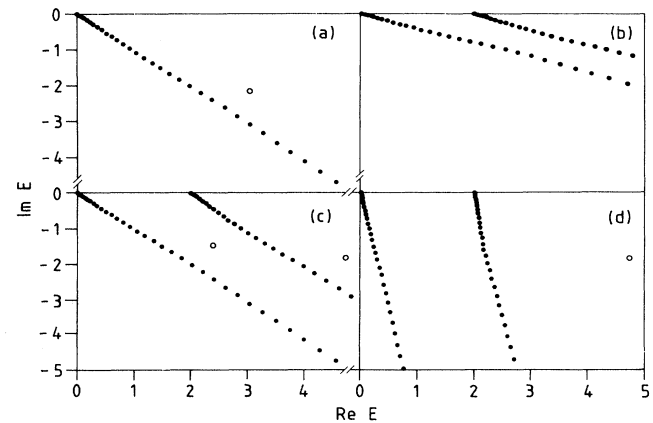


FIG. 1. Energy eigenvalues of (a) a one-channel problem with a one-term separable potential ( $\lambda_{11} = 1.0$ ) and (b)–(d) a two-channel problem with one-term separable potentials ( $\lambda_{11} = 1.0$ ,  $\lambda_{22} = 0.0$ ,  $\lambda_{12} = \lambda_{21} = 1.0$ , and  $E_2 = 2$ ). The dots are the points of the rotated discretized continua, while the circles are the poles of the  $S$  matrix on different Riemann sheets. The rotation angles (in rad) are (a) 0.4, (b) 0.2, (c) 0.4, and (d) 0.7.

and has not been swept over by any other ones. From this it follows that one can imagine situations where a shadow pole can be revealed only if the rotation angles in different channels are different. For instance, to reveal a pole above the first channel threshold on the  $(+)$  sheet, the rotation angle in the second channel must be greater than the one in the first channel. It is questionable whether the CSM can cope with such a constraint. The theory of the multichannel CSM always assumes that  $\theta$  is the same for all channels. Here, just to see what happens, we venture to choose two different  $\theta$ .

It seems natural to generalize the multichannel complex-scaling transformation (5) in the following way:

$$\widehat{U}_{\alpha\beta} = \delta_{\alpha\beta} \widehat{U}_{\alpha}(\theta_{\alpha}). \quad (8)$$

In the coordinate space the action of  $\widehat{U}_{\alpha}(\theta_{\alpha})$  is

$$\widehat{U}_{\alpha}(\theta_{\alpha})f(r) = e^{3i\theta_{\alpha}/2} f(re^{i\theta_{\alpha}}). \quad (9)$$

This definition ensures that the  $\{\widehat{U}_{\alpha\beta}\}$  operator matrix inherits all properties of  $\widehat{U}(\theta)$ . Applying the transformation (8) to the Hamiltonian of Eq. (4), we arrive at

$$\sum_{\beta=1}^N \widehat{U}_{\alpha}(\theta_{\alpha}) \widehat{H}_{\alpha\beta} \widehat{U}_{\beta}^{-1}(\theta_{\beta}) |\Psi_{\theta_{\beta}}^{\beta}\rangle = E_{\theta_{\alpha}, \theta_{\beta}}^{\alpha} |\Psi_{\theta_{\alpha}}^{\alpha}\rangle, \quad \alpha = 1, 2, \dots, N. \quad (10)$$

As an illustrative example, we write down the function  $\widehat{U}_{\alpha}(\theta_{\alpha}) \widehat{H}_{\alpha\beta} \widehat{U}_{\beta}^{-1}(\theta_{\beta}) |\Psi_{\theta_{\beta}}^{\beta}\rangle$  and its overlap with the function  $\langle \Psi_{\theta_{\alpha}}^{\alpha} |$  in the coordinate space. If the operator  $\widehat{H}_{\alpha\beta}$  connects channels which have the same dynamical coordinate  $r$ , then

$$\langle r | \widehat{U}_{\alpha}(\theta_{\alpha}) \widehat{H}_{\alpha\beta} \widehat{U}_{\beta}^{-1}(\theta_{\beta}) |\Psi_{\theta_{\beta}}^{\beta}\rangle = e^{3i(\theta_{\alpha}-\theta_{\beta})/2} H_{\alpha\beta}(re^{i\theta_{\alpha}}) \Psi_{\theta_{\beta}}^{\beta}(re^{i(\theta_{\alpha}-\theta_{\beta})}), \quad (11)$$

and

$$\begin{aligned} & \langle \Psi_{\theta_{\alpha}}^{\alpha} | \widehat{U}_{\alpha}(\theta_{\alpha}) \widehat{H}_{\alpha\beta} \widehat{U}_{\beta}^{-1}(\theta_{\beta}) |\Psi_{\theta_{\beta}}^{\beta}\rangle \\ &= e^{-3i(\theta_{\alpha}+\theta_{\beta})/2} \\ & \times \int \Psi_{\theta_{\alpha}}^{\alpha}(re^{-i\theta_{\alpha}}) H_{\alpha\beta}(r) \Psi_{\theta_{\beta}}^{\beta}(re^{-i\theta_{\beta}}) r^2 dr. \quad (12) \end{aligned}$$

If the  $\widehat{H}_{\alpha\beta}$  operator connects rearrangement channels with the dynamical coordinates  $r_{\alpha}$  and  $r_{\beta}$  [i.e., in the coordinate space  $\widehat{H}_{\alpha\beta}f(r_{\beta}) = \int dr_{\beta} r_{\beta}^2 H_{\alpha\beta}(r_{\alpha}, r_{\beta}) f(r_{\beta})$ ], then

$$\begin{aligned} & \langle r_{\alpha} | \widehat{U}_{\alpha}(\theta_{\alpha}) \widehat{H}_{\alpha\beta} \widehat{U}_{\beta}^{-1}(\theta_{\beta}) |\Psi_{\theta_{\beta}}^{\beta}\rangle \\ &= e^{3i(\theta_{\alpha}-\theta_{\beta})/2} \\ & \times \int H_{\alpha\beta}(r_{\alpha}e^{i\theta_{\alpha}}, r_{\beta}) \Psi_{\theta_{\beta}}^{\beta}(r_{\beta}e^{-i\theta_{\beta}}) r_{\beta}^2 dr_{\beta}, \quad (13) \end{aligned}$$

and

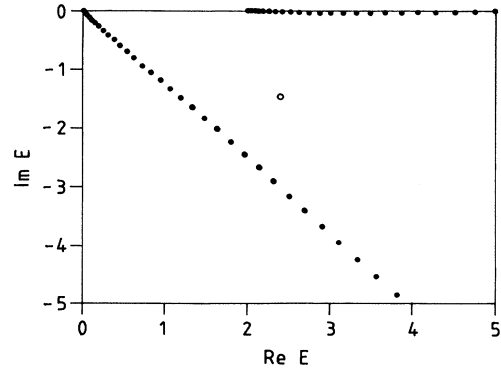


FIG. 2. Energy eigenvalues of the two-channel problem of Fig. 1. The rotation angles are  $\theta_1 = 0.45$  and  $\theta_2 = 0$ .

$$\begin{aligned} & \langle \Psi_{\theta_{\alpha}}^{\alpha} | \widehat{U}_{\alpha}(\theta_{\alpha}) \widehat{H}_{\alpha\beta} \widehat{U}_{\beta}^{-1}(\theta_{\beta}) |\Psi_{\theta_{\beta}}^{\beta}\rangle \\ &= e^{-3i(\theta_{\alpha}+\theta_{\beta})/2} \int \int \Psi_{\theta_{\alpha}}^{\alpha}(r_{\alpha}e^{-i\theta_{\alpha}}) H_{\alpha\beta}(r_{\alpha}, r_{\beta}) \\ & \quad \times \Psi_{\theta_{\beta}}^{\beta}(r_{\beta}e^{-i\theta_{\beta}}) r_{\alpha}^2 dr_{\alpha} r_{\beta}^2 dr_{\beta}. \quad (14) \end{aligned}$$

Deriving (12) and (14) the Cauchy theorem was used, assuming that all potential operators are analytic [like ours, (6)]. We can see that the matrix elements of the transformed operator  $\widehat{U}_{\alpha}(\theta_{\alpha}) \widehat{H}_{\alpha\beta} \widehat{U}_{\beta}^{-1}(\theta_{\beta})$  between the original channel states  $|\Psi_{\theta_{\alpha}}^{\alpha}\rangle$  and  $|\Psi_{\theta_{\beta}}^{\beta}\rangle$  can be expressed as the matrix elements of the original operator  $\widehat{H}_{\alpha\beta}$  between the so-called back-rotated channel states. This is a well-known feature of the usual complex-scaling method, too.

We tested this generalized CSM with the above two-channel problem setting  $\theta_2 = 0$ . The result is in Fig. 2. The position of the  $(-)$  shadow pole remains the same as it was in Fig. 1 within 7 decimal digits, which is a

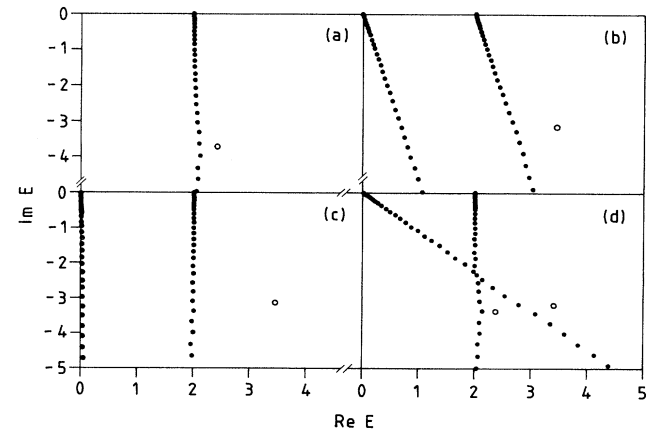


FIG. 3. The same as Fig. 1, with the potential strengths (a)  $\lambda_{22} = 0.2$ ; (b)-(d)  $\lambda_{11} = 0.0$ ,  $\lambda_{22} = 0.2$ , and  $\lambda_{12} = \lambda_{21} = 0.42$ . The rotation angles are (a) 0.78, (b) 0.68, (c) 0.78, and (d)  $\theta_1 = 0.42$ ,  $\theta_2 = 0.78$ .

remarkable stability regarding that no optimization was made in  $\bar{b}$  and  $\theta_1$ .

The really relevant test is, however, an example where there is a shadow pole on  $(+-)$ . To achieve this, we set  $\lambda_{22} = 0.2$ , which, in a one-channel problem, results in a pole at  $2.430 - i3.704$  [Fig. 3(a)]. Switching on the coupling ( $\lambda_{12} = \lambda_{21} = 0.42$ ), figures similar to Fig. 1 can be generated [Figs. 3(b)–3(d)]. Now the pole at  $3.381 - i3.228$  is revealed when both channel continua have swept over this point, so that this pole is on the  $(--)$  sheet. The other pole at  $2.373 - i3.357$  is revealed when the continuum of the second channel has swept over it and that of the first one has not, which shows that this pole is a shadow pole on the  $(+-)$  sheet, in agreement with the fact that these poles originate from the second channel [9]. In this example the variation of the rotation angles slightly removes the poles from their original positions. This is, however, certainly caused by the fact that, because of the unlucky location of the poles, we have to choose rotation angles that are far from optimum. If we do not want to reveal the two poles at the same time, we can optimize the  $\theta$  angles, which results in stable pole positions.

Finally, we mention an interesting feature of the

present method. Let us suppose that there is a multichannel problem where there are degenerate thresholds. Then some of the Riemann sheets cannot be reached from the physical sheet by following analytical continuation paths because one cannot pass between two thresholds that coincide. Using the above multichannel CSM with different rotation angles in these channels, we can reach such Riemann sheets.

In summary, we have investigated the applicability of the multichannel complex-scaling method to explore the pole structure in multichannel scattering problems. We have used a natural extension of the single-channel complex-scaling transformation to multichannel cases, which allows us to find the poles of the scattering matrix on all Riemann sheets. We have found that this extension works as expected and is able to find all conventional poles and shadow poles reliably.

This research was supported by OTKA (National Science Research Foundation, Hungary) under Contract No. 3010. The author is indebted to Professor B. Gyarmati and Professor R. G. Lovas for stimulating discussions and for reading the manuscript.

---

\* Electronic address: H988CSO@HUELLA.BITNET

- [1] A. J. F. Siegert, *Phys. Rev.* **56**, 750 (1939).
- [2] Y. K. Ho, *Phys. Rep.* **99**, 1 (1983), and references therein.
- [3] N. Moiseyev, P. R. Certain, and F. Weinhold, *Mol. Phys.* **36**, 1613 (1978); *Proceedings of the Sanibel Workshop Complex Scaling, 1978* [*Int. J. Quantum Chem.* **14**, 343 (1978)]; B. R. Junker, *Adv. At. Mol. Phys.* **18**, 207 (1982).
- [4] W. P. Reinhardt, *Annu. Rev. Phys. Chem.* **33**, 223 (1982).
- [5] *Resonances—The Unifying Route Towards the Formulation of Dynamical Processes, Foundations and Applications in Nuclear, Atomic and Molecular Physics*, edited by E. Brändas and N. Elander, *Lecture Notes in Physics* Vol. 325 (Springer-Verlag, Berlin, 1989).
- [6] A. T. Kruppa, R. G. Lovas, and B. Gyarmati, *Phys. Rev. C* **37**, 383 (1988).
- [7] A. T. Kruppa and K. Katō, *Prog. Theor. Phys.* **84**, 1145 (1990).
- [8] R. J. Eden and J. R. Taylor, *Phys. Rev.* **133**, B1575 (1964).
- [9] B. C. Pearce and B. F. Gibson, *Phys. Rev. C* **40**, 902 (1989).
- [10] A. Csótó, R. G. Lovas, and A. T. Kruppa, *Phys. Rev. Lett.* **70**, 1389 (1993).
- [11] R. M. Potvliege and R. Shakeshaft, *Phys. Rev. A* **38**, 6190 (1988); M. Dörr and R. M. Potvliege, *ibid.* **41**, 1472 (1990).
- [12] D. Morgan and M. R. Pennington, *Phys. Rev. Lett.* **59**, 2818 (1987); *Phys. Lett. B* **258**, 444 (1991); F. Cannata, J. P. Dedonder, and L. Leśniak, *Z. Phys. A* **343**, 451 (1992).
- [13] G. M. Hale, R. E. Brown, and N. Jarmie, *Phys. Rev. Lett.* **59**, 763 (1987); L. N. Bogdanova, G. M. Hale, and V. E. Markushin, *Phys. Rev. C* **44**, 1289 (1991).
- [14] P. O. Löwdin, *Adv. Quantum Chem.* **19**, 87 (1988).
- [15] J. Aguilar and J. M. Combes, *Commun. Math. Phys.* **22**, 269 (1971); E. Balslev and J. M. Combes, *ibid.* **22**, 280 (1971); B. Simon, *ibid.* **27**, 1 (1972).
- [16] E. Brändas, M. Rittby, and N. Elander, in *Resonances—The Unifying Route Towards the Formulation of Dynamical Processes, Foundations and Applications in Nuclear, Atomic and Molecular Physics*, edited by E. Brändas and N. Elander, *Lecture Notes in Physics* Vol. 325 (Springer-Verlag, Berlin, 1989), p. 345.
- [17] A. Csótó, B. Gyarmati, A. T. Kruppa, K. F. Pál, and N. Moiseyev, *Phys. Rev. A* **41**, 3469 (1990).
- [18] A. Csótó, B. Gyarmati, and A. T. Kruppa, *Few-Body Systems* **11**, 149 (1991).